J|A|C|S
ARTICLES
Published on Web 04/03/2007

Kinetic and Computational Analysis of the Palladium(II)-Catalyzed Asymmetric Allylic Trichloroacetimidate Rearrangement: Development of a Model for Enantioselectivity

Mary P. Watson,[†] Larry E. Overman,*[,†] and Robert G. Bergman*[,‡]

Contribution from the Department of Chemistry, 1102 Natural Sciences II, University of California, Irvine, California 92697-2025, and Department of Chemistry, University of California, and Division of Chemical Sciences, Lawrence Berkeley National Laboratory, Berkeley, California 94720

Received October 27, 2006; E-mail: leoverma@uci.edu

Abstract: The asymmetric rearrangement of allylic trichloroacetimidates catalyzed by palladium(II) complexes of the COP family is a powerful method for the preparation of enantioenriched chiral allylic amines from prochiral allylic alcohols. A detailed kinetic analysis of this reaction was performed to elucidate the rate- and enantiodetermining step of this important reaction. The results of these studies support a cyclization-induced rearrangement mechanism and prompted DFT studies (B3LYP/LACVP**+) of C−N bond formation, believed to be the enantiodetermining step of this catalytic cycle. On the basis of these calculations, a model for enantioinduction was developed, in which the planar chirality of the catalyst controls the enantioselectivity. These studies should allow the rational design of more enantioselective catalysts.

Introduction

With the recent development of a chiral, nonracemic palladium(II) catalyst for the asymmetric allylic trichloroacetimidate rearrangement,[1] a powerful method for the preparation of chiral allylic amines from achiral allylic alcohols is now available. This practical method relies on COP-based dimer and monomer catalysts **5** (Scheme 1).[2,3] Although other chiral palladium(II) catalysts have been successfully used to catalyze the asymmetric rearrangement of protected allylic *N*-(*p*-methoxyphenyl)trifluoroacetimidates and *N*-arylbenzimidates,[4] $[COP\text{-}Cl]_2$, $[COP\text{-}Br]_2$, COP-hfacac, and COP-acac are the only chiral catalysts reported to date that efficiently catalyze the rearrangement of allylic trichloroacetimidates **2**. In an effort to understand why these COP-based compounds are efficient catalysts for the rearrangement of unprotected allylic trichloroacetimidates, mechanistic analysis of this catalytic asymmetric rearrangement was undertaken.

Scheme 1. Preparation of Chiral Amines by the COP-Catalyzed Allylic Trichloroacetimidate Rearrangement

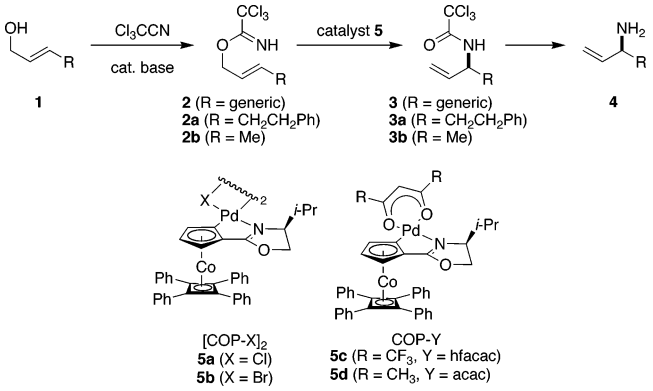

The generally accepted mechanism for the palladium(II)-catalyzed allylic imidate rearrangement is a cyclization-induced rearrangement (Scheme 2).[1,5] In this pathway, palladium coordination activates the double bond toward nucleophilic attack by the imidate nitrogen. Cyclization of π-complex **7** provides alkylpalladium intermediate **8**.[6] Grob-like fragmentation then leads to palladium-bound unsaturated amide **9**. Displacement of the amide from palladium then releases product **10**.

[†] University of California, Irvine, California.

[‡] University of California and Division of Chemical Sciences, Lawrence Berkeley National Laboratory, Berkeley.

(1) For a recent comprehensive review, see: Overman, L. E.; Carpenter, N. E. In *Organic Reactions*; Overman, L. E., Ed.; Wiley: Hoboken, NJ, 2005; Vol. 66, pp 1−107.

(2) (a) Anderson, C. E.; Overman, L. E. *J. Am. Chem. Soc.* **2003**, *125*, 12412−12413. (b) Kirsch, S. F.; Overman, L. E.; Watson, M. P. *J. Org. Chem.* **2004**, *69*, 8101−8104.

(3) $[COP\text{-}Cl]_2$ (**5a**) = di-μ-chlorobis[(η^5-(*S*)-(*pR*)-2-(2′-(4′-methylethyl)oxazolinyl)cyclopentadienyl, 1-*C*, 3′-*N*)(η^4-tetraphenylcyclobutadiene)cobalt]-dipalladium. This catalyst is commercially available from Aldrich.

(4) (a) Donde, Y.; Overman, L. E. *J. Am. Chem. Soc.* **1999**, *121*, 2933−2934. (b) Calter, M.; Hollis, T. K.; Overman, L. E.; Ziller, J.; Zipp, G. G. *J. Org. Chem.* **1997**, *62*, 1449−1456. (c) Hollis, T. K.; Overman, L. E. *Tetrahedron Lett.* **1997**, *38*, 8837−8840. (d) Jiang, Y.; Longmire, J. M.; Zhang, X. *Tetrahedron Lett.* **1999**, *40*, 1449−1450. (e) Uozumi, Y.; Kato, K.; Hayashi, T. *Tetrahedron: Asymmetry* **1998**, *9*, 1065−1072. (f) Cohen, F.; Overman, L. E. *Tetrahedron: Asymmetry* **1998**, *9*, 3213−3222. (g) Kang, J.; Yew, K. H.; Kim, T. H.; Choi, D. H. *Tetrahedron Lett.* **2002**, *43*, 9509−9512. (h) Leung, P.-H.; Ng, K.-H.; Li, Y.; White, A. J. P.; Williams, D. J. *Chem. Commun.* **1999**, 2435−2436. (i) Overman, L. E.; Owen, C. E.; Pavan, M. M.; Richards, C. J. *Org. Lett.* **2003**, *5*, 1809−1812.

(5) Overman, L. E. *Angew. Chem., Int. Ed. Engl.* **1984**, *23*, 579−586 and references therein.

(6) Alkylpalladium complex **8** may also be a transition state, instead of an intermediate. Prior to these studies, the intermediacy of this complex had not been investigated.

Scheme 2. Cyclization-Induced Rearrangement Mechanism

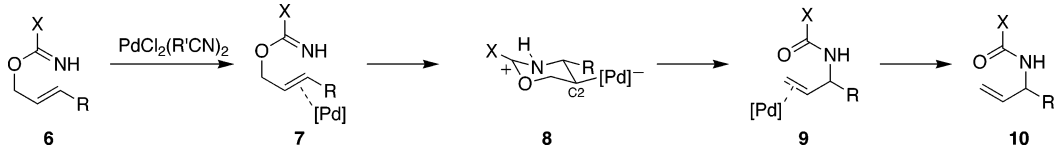

Scheme 3. Possible Pathways for the Cyclization-Induced Rearrangement of Homochiral Secondary Allylic Imidates

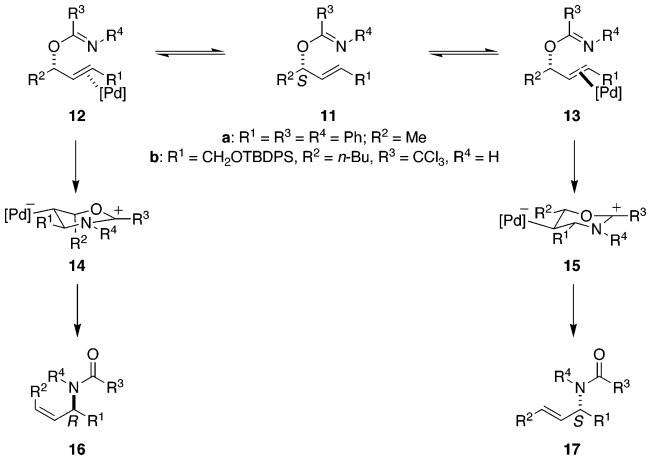

Previous observations with achiral palladium(II) catalysts support a cyclization-induced rearrangement mechanism for [3,3]-sigmatropic rearrangements of allylic imidates and related allylic esters and carbamates.[1,5,7] First, byproducts from allyl cation or η^3-allylpalladium intermediates are not observed when palladium(II) compounds are used as catalysts. In contrast, palladium(0) and platinum(0) catalysts do give these byproducts.[8] A concerted charge-induced rearrangement can also be discounted, because soft electrophiles such as palladium(II) and mercury(II) are more effective catalysts than hard Lewis or Brønsted acids.[5] Additionally, this rearrangement typically does not occur if there is substitution at C2. This observation is consistent with formation of a carbon−palladium σ-bond at C2; the C2 substituent sterically hinders formation of alkylpalladium intermediate **8**. Finally, the rate of the palladium(II)-catalyzed allylic imidate rearrangement increases as the electron-donating ability of X increases ($X = NR_2 > OR > CH_3 > CF_3$). This latter fact indicates that positive charge accumulates on the imidate carbon during the reaction.[1]

Although these observations support the cyclization-induced mechanism, there have been no kinetic studies to confirm this mechanism or to ascertain the rate-determining step of this reaction with either achiral or chiral palladium(II) catalysts. The rate-determining step could be either palladium−olefin coordination to form intermediate **7** or C−N bond formation to give intermediate **8**. In 1997, Hollis and Overman proposed that the enantio- and rate-determining step may depend on the nucleophilicity of the imidate nitrogen (Scheme 3).[9] Because the rearrangement of electron-poor trichloroacetimidate **11b** led exclusively to amide **17**,[10] they argued that C−N bond formation must be enantiodetermining. In this case, the product ratio is governed by the energy difference between the six-membered, envelope transition states that lead to intermediates **14** and **15**. The pathway to intermediate **15** is favored, because all substituents are in pseudoequatorial positions. In contrast, rearrangement of electron-rich benzimidate **11a** provided a 1:4 ratio of products **16** and **17**.[8] In this case, it was proposed that the more electron-rich benzimidate cyclized more quickly, thereby making olefin−palladium coordination the enantiodetermining step. Although the differing reactivity of imidates **11a** and **11b** is suggestive of a difference in enantio- and rate-determining steps, no further studies have been conducted to confirm this hypothesis in either asymmetric or nonasymmetric allylic imidate rearrangements.

To explore the mechanism of the palladium(II)-catalyzed asymmetric allylic trichloroacetimidate rearrangement, kinetic studies of the $[COP\text{-}Cl]_2$-catalyzed allylic trichloroacetimidate rearrangement were conducted. In the course of this research, the reactivity difference between *E* and *Z* allylic trichloroacetimidates was also explored. Additionally, discovery of a nitrogen-bound palladium−imidate adduct was made. In addition to kinetic studies, computational modeling of the cyclization-induced rearrangement was performed.[11] These DFT calculations support the cyclization-induced rearrangement mechanism and allowed development of a model for the enantioselectivity provided by $[COP\text{-}Cl]_2$.[12,13] These results should enable the rational design of more selective COP-based catalysts.

Results

1. Kinetic Studies Using Dichloropalladate 5e. An extensive search for a monomeric COP-based model catalyst appropriate for kinetic studies led to our selection of dichloropalladate **5e** as a suitable candidate for detailed investigation. Dichloropalladate **5e** can be formed in situ by addition of tetrabutylammonium chloride to a solution of $[COP\text{-}Cl]_2$ and CD_2Cl_2 (eq 1).[14]

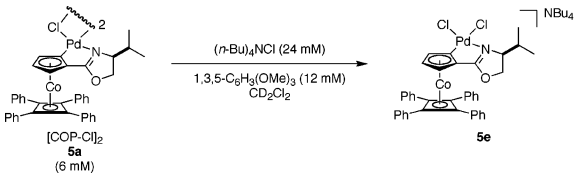

(1)

This dichloropalladate efficiently catalyzes the rearrangement

(7) Overman, L. E.; Campbell, C. B.; Knoll, F. M. *J. Am. Chem. Soc.* **1978**, *100*, 4822−4834.
(8) Schenck, T. G.; Bosnich, B. *J. Am. Chem. Soc.* **1985**, *107*, 2058−2066.
(9) Hollis, T. K.; Overman, L. E. *J. Organomet. Chem.* **1999**, *576*, 290−299.
(10) Mehmandoust, M.; Petit, Y.; Larchevêque, M. *Tetrahedron Lett.* **1992**, *33*, 4313−4316.
(11) The thermal diastereoselective allylic trichloroacetimidate rearrangement has been computationally studied using semiempirical methods. See: Eguchi, T.; Koudate, T.; Kakinuma, K. *Tetrahedron* **1993**, *49*, 4527−4540.
(12) Previous to this work, a model for the enantioinduction of the $[COP\text{-}OCOCF_3]_2$-catalyzed allylic *N*-(*p*-methoxyphenyl)benzimidate rearrangement was proposed. See: Kang, J.; Kim, T. H.; Yew, K. H.; Lee, W. K. *Tetrahedron: Asymmetry* **2003**, *14*, 415−418.
(13) After the present study was completed, the Peters research group published a model for the enantioselectivity observed in the allylic *N*-(*p*-methoxyphenyl)trifluoroacetimidate rearrangement catalyzed by a palladium(II) compound with a ferrocenium-based chiral ligand. Their model is based upon structure−activity relationships of systematically varied catalysts. See: Weiss, M. E.; Fischer, D. F.; Xin, Z.-Q.; Jautze, S.; Schweizer, W. B.; Peters, R. *Angew. Chem., Int. Ed.* **2006**, *45*, 5694−5698.
(14) 1,3,5-Trimethoxybenzene was used as an NMR internal standard.

Scheme 4. Cyclization-Induced Rearrangement Mechanism for COP-Based Catalysts

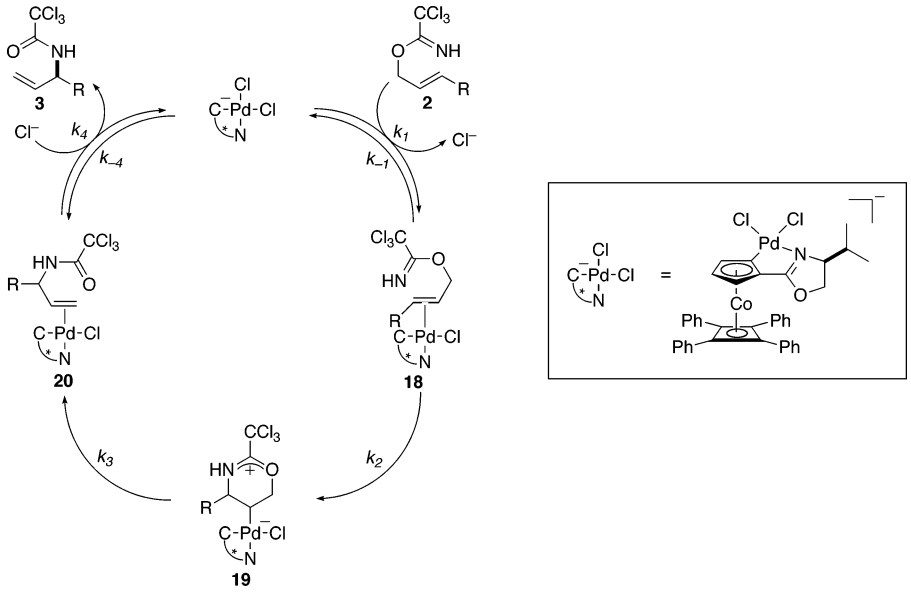

of allylic trichloroacetimidate **2a**, providing **3a** with the same high enantiopurity as $[COP\text{-}Cl]_2$ (Scheme 1).[2a]

With the use of dichloropalladate **5e**, insight into the rate-determining step of the allylic trichloroacetimidate rearrangement would be provided by the rate dependence on chloride concentration (Scheme 4). In the cyclization-induced rearrangement mechanism, coordination of olefin **2** displaces chloride from dichloropalladate **5e**. Subsequently, nitrogen attacks the activated olefin to produce cyclic intermediate **19**. Assuming that the fragmentation of alkylpalladium intermediate **19** is rapid,[15,16] a rate law for this mechanism can be represented as shown in eq 2. There are two limiting cases for this mechanism. If palladium−olefin coordination is rate-determining ($k_2 \gg k_{-1}[Cl^-]$), then the rate will show no dependence on chloride concentration, and the rate equation can be simplified to eq 3.[17] In the second possibility, in which C−N bond formation is rate-determining ($k_{-1}[Cl^-] \gg k_2$), the rate will depend on the chloride concentration, and the rate law can be represented as eq 4. Based on this hypothesis, we determined the kinetics of the COP dichloropalladate-catalyzed allylic trichloroacetimidate rearrangement in an effort to understand the rate-limiting step of the catalytic cycle. In these studies, allylic trichloroacimidate **2a** was used as the substrate and tetrabutylammonium chloride as the chloride source.

$$\text{rate} = \frac{k_1 k_2[\mathbf{5e}][\mathbf{2}]}{k_{-1}[Cl^-] + k_2} \tag{2}$$

$$\text{rate} = k_1[\mathbf{5e}][\mathbf{2}] \tag{3}$$

$$\text{rate} = \frac{k_1 k_2[\mathbf{5e}][\mathbf{2}]}{k_{-1}[Cl^-]} \tag{4}$$

The allylic trichloroacetimidate rearrangement displayed first-order rate dependence on the concentration of trichloroacetimidate **2a** (R = CH_2CH_2Ph). For every reaction, the trichloroacetimidate decay was fit well by the first-order decay function.[18,19] In addition, the observed rate constant did not change when the initial concentration of trichloroacetimidate **2a** was increased 4-fold. The concentration of amide **3a** increased proportionally to imidate decay and was fit well by the first-order growth function.[18] This observation suggests that reaction intermediates do not accumulate substantially during the catalytic cycle. The detailed kinetic data are provided as Supporting Information.

First-order rate dependence on the concentration of dichloropalladate **5e** was also observed. With the use of the same concentrations of trichloroacetimidate **2a** (111 mM) and excess tetrabutylammonium chloride (54.0 mM), the concentration of dichloropalladate catalyst **5e** was varied from 10.7−33.7 mM. The observed rate constant increased linearly with increasing concentration of palladate **5e**, supporting first-order rate dependence on the concentration of the palladium catalyst.

The impact of ionic strength on reaction rate was also determined. Addition of varying concentrations of tetrabutylammonium hexafluorophosphate to the rearrangement of trichloroacetimidate **2a** catalyzed by dichloropalladate **5e** had no effect

(15) We make the assumption that fragmentation of alkylpalladium intermediate **19** is rapid based on the exothermicity of the overall reaction, which is thermodynamically favored by approximately 14 kcal/mol (see ref 16). If formation of alkylpalladium intermediate **19** were rate-determining, then its fragmentation to form the C=O bond will have an early transition state, close in energy to intermediate **19**. Our computations (discussed below) are in agreement with this assumption. Alternatively, we could assume that formation of η^2-(alkene)palladium intermediate **20** is the first irreversible step. This would add a k_3 term to our general rate law but would not alter the rate dependence on catalyst, imidate, or chloride.

(16) Conversion of the imidate to the amide is thermodynamically favored by about 14 kcal/mol. See: (a) Beak, P.; Bonham, J.; Lee, J. T. *J. Am. Chem. Soc.* **1968**, *90*, 1569−1582. (b) Beak, P. *Acc. Chem. Res.* **1977**, *10*, 186−192. (c) Beak, P.; Lee, J.-K.; Zeigler, J. M. *J. Org. Chem.* **1978**, *43*, 1536−1538.

(17) This analysis assumes that olefin displaces chloride in an associative manner. Another possibility is reversible dissociation of chloride followed by palladium−olefin coordination in an independent elementary step. This mechanism is unlikely, because ligand dissociation from a 16-electron palladium(II) complex creates a 14-electron, coordinatively unsaturated intermediate. In general, associative pathways for ligand substitution are strongly favored for palladium(II) complexes. See: Crabtree, R. H. *The Organometallic Chemistry of the Transition Metals*, 2nd ed.; John Wiley & Sons, Inc.: New York, 1994; pp 89−90.

(18) Nonlinear decay and growth curves were fit using: *KaleidaGraph*, version 3.6.; Synergy Software: Reading, PA, 2003.

(19) Espenson, J. H. *Chemical Kinetics and Reaction Mechanisms*; McGraw-Hill, Inc.: New York, 1995; p 23.

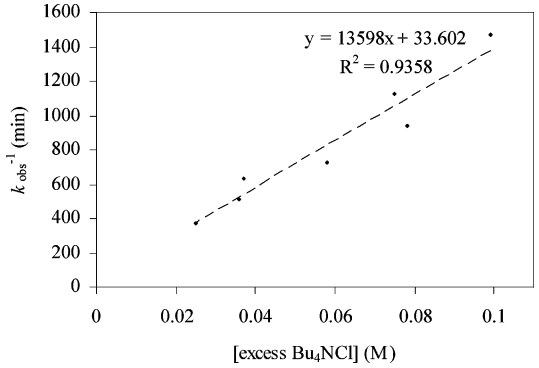

Figure 1. The inverse of the observed rate constant (k_{obs}^{-1}) vs the concentration of excess tetrabutylammonium chloride. Conditions: imidate **2a** (99.5 mM), dichloropalladate **5e** (17.7 mM), excess tetrabutylammonium chloride, trimethoxybenzene (12 mM), CD_2Cl_2, 60 °C.

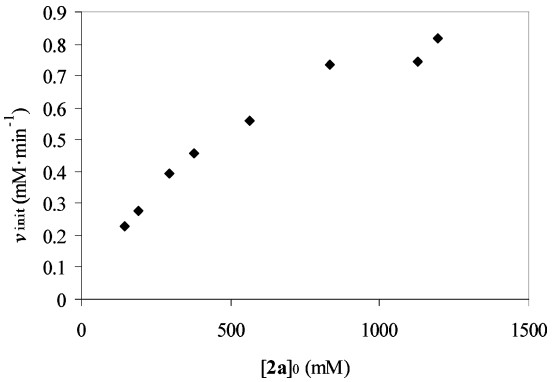

Figure 2. Initial rates vs initial concentration of imidate **2a**. Conditions: $[COP\text{-}Cl]_2$ (6 mM), imidate **2a**, 1,3,5-trimethoxybenzene (30 mM), CD_2Cl_2, 310 K.

on the reaction rate.[20] Thus, the reaction rate is not affected by the ionic strength of the solution.

The rearrangement rate displayed an inverse dependence on the concentration of tetrabutylammonium chloride. A linear relationship was observed between the concentration of tetrabutylammonium chloride and the inverse of the observed rate constant (Figure 1). As shown by the rearrangement of eq 2 to eq 5, this linear relationship supports the conclusion that reversible chloride dissociation occurs before the rate-limiting step.

$$\frac{1}{k_{obs}} = \left(\frac{k_{-1}}{k_1 k_2[\mathbf{5e}]}\right)[Bu_4NCl] + \frac{1}{k_1[\mathbf{5e}]} \qquad (5)$$

2. $[COP\text{-}Cl]_2$-Catalyzed Rearrangement. 2.1 Kinetic Studies. Reversible dissociation of chloride before the rate-determining step suggests that palladium−olefin coordination might also be reversible. To investigate this hypothesis, the kinetics of the $[COP\text{-}Cl]_2$-catalyzed rearrangement of trichloroacetimidate **2a** were investigated. At constant concentrations of $[COP\text{-}Cl]_2$ (6 mM), the reaction rate displayed saturation behavior with increasing initial concentrations of trichloroacetimidate **2a**, as shown in Figure 2 and the corresponding Hanes−Woolf plot (Figure 3).[21] Observation of saturation kinetics indicates that

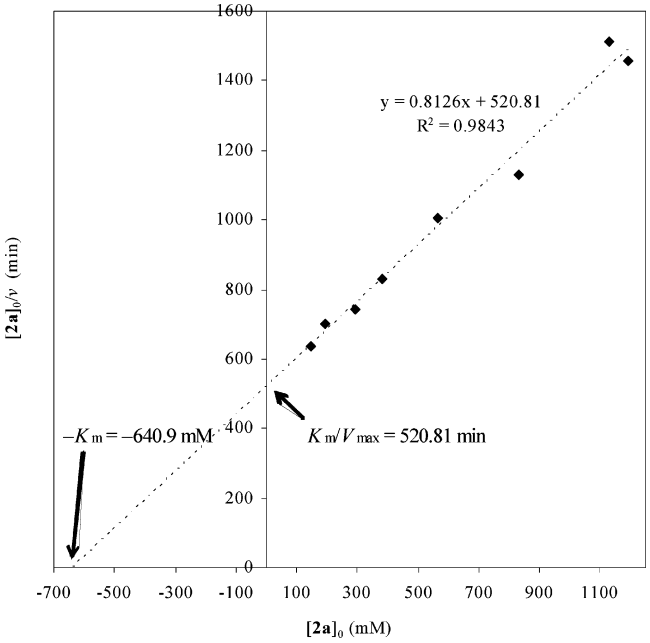

Figure 3. Hanes−Woolf plot showing saturation with imidate **2a**. K_m = 640.9 mM. V_{max} = 1.23 mM·min^{-1}. Conditions: $[COP\text{-}Cl]_2$ (6 mM), imidate **2a**, 1,3,5-trimethoxybenzene (30 mM), CD_2Cl_2, 310 K.

trichloroacetimidate **2a** reacts with $[COP\text{-}Cl]_2$ at high concentrations to reversibly form a catalyst−imidate complex (**21**, eq 6).

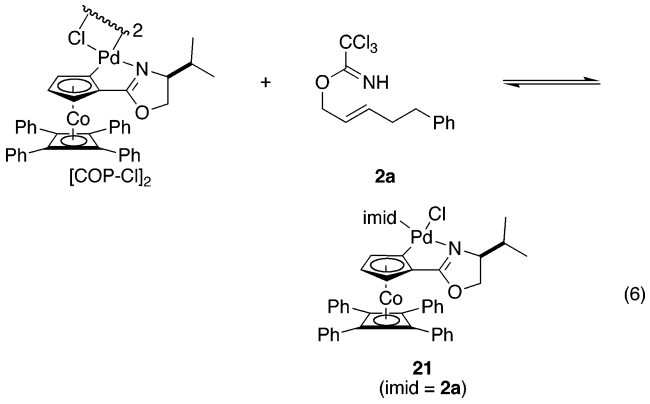

(6)

This catalyst−imidate complex can be observed by mass spectrometry and ^1H NMR spectroscopy. In the high-resolution mass spectrum of a solution of $[COP\text{-}Cl]_2$ and allylic trichloroacetimidate **2a**, a peak at 1003.1069 was observed. This mass corresponds to the mass of complex **21** less chloride [1003.1069 calcd for $C_{52}H_{47}Cl_3CoN_2O_2Pd$; (M − Cl)]. By ^1H NMR spectroscopy, $[COP\text{-}Cl]_2$ was observed as the catalyst resting state at low initial concentrations of trichloroacetimidate **2a**. However, at high concentrations of trichloroacetimidate **2a**, a new catalyst resting state (**21**) was observed at the beginning of the reaction. As the reaction progressed, this species gradually disappeared and a catalyst−amide complex developed. In an independent experiment, addition of amide **3a** to a solution of $[COP\text{-}Cl]_2$ and CD_2Cl_2 resulted in formation of the same compound, as determined by ^1H NMR spectroscopy.

The rate dependence on the concentration of catalyst−imidate complex **21** was studied under saturation conditions. With the use of a constant concentration of trichloroacetimidate **2a** (1.2 M), the initial rate displayed a first-order dependence on the

(20) The concentration of tetrabutylammonium hexafluorophosphate was varied from 12−48 mM at constant concentrations of imidate **2a** (117 mM), dichloropalladate **5e** (9.0 mM), and tetrabutylammonium chloride (24 mM).
(21) Silverman, R. B. *The Organic Chemistry of Enzyme-Catalyzed Reactions*; Academic Press: San Francisco, CA, 2000; pp 563−596.

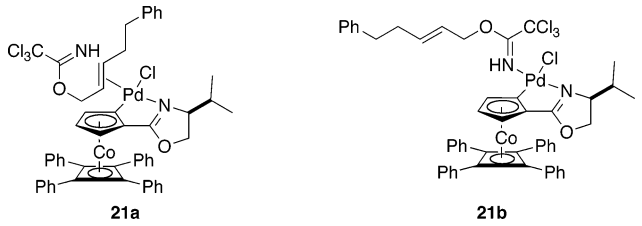

Figure 4. Possible structures of catalyst−imidate complex **21**.

concentration of the catalyst−imidate complex (see data in the Supporting Information), which was the only catalyst species observed by ^{1}H NMR over the time course measured in these initial rate studies.

2.2. Structure of Catalyst−Imidate Complex 21. Because a large excess of trichloroacetimidate **2a** was needed to form complex **21** in situ, the structure of catalyst−imidate complex **21** was not easily determined by ^{1}H NMR spectroscopy. To investigate whether alkene-bound palladium complex **21a** or nitrogen-bound palladium adduct **21b** was the catalyst resting state under saturation conditions, several model substrates were studied (Figure 4).

Insight into the binding mode was provided by using saturated trichloroacetimidate **22**. Treatment of $[COP\text{-}Cl]_2$ with an excess of trichloroacetimidate **22** resulted in formation of complex **23** (eq 7). The approximate equilibrium constant of this reaction

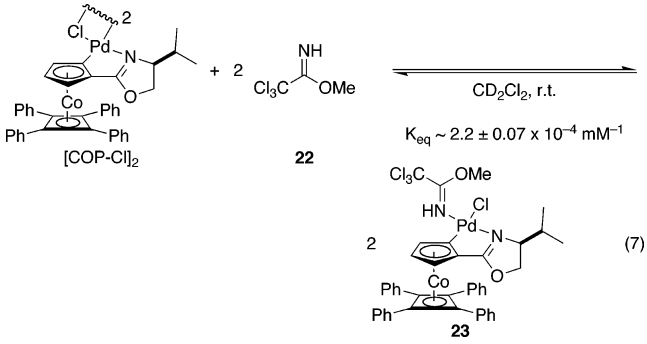

is 2.2×10^{-4} mM^{-1}. Because it could only be formed in the presence of a large excess of trichloroacetimidate **22**, the structure of imidate-bound palladium complex **23** was studied by a series of NMR spectroscopy experiments. With the use of diffusion-ordered spectroscopy (DOSY), the ^{1}H NMR peaks of compound **23** could be separated from that of unbound imidate **22**. With the use of both HMQC and HMBC experiments, all protons and carbons of complex **23** could be assigned. The sp^2 imidate carbon of the bound imidate is shifted upfield from those in the unbound imidate (166.2 vs 163.2 ppm, respectively). Additionally, the nitrogen-bound hydrogen of the coordinated imidate was located by HMBC (7.7 ppm), indicating that the imidate is not deprotonated upon binding palladium. Unfortunately, no HMBC cross-peaks were observed between the bound imidate and the COP ligand.

trans-2-Pentene was used as a model for the olefin portion of allylic trichloroacetimidate **2a**. When *trans*-2-pentene (2.3 M), $[COP\text{-}Cl]_2$ (30 mM), and CD_2Cl_2 were combined, only traces of a new complex were observed by ^{1}H NMR spectroscopy (eq 8). $[COP\text{-}Cl]_2$ was the major COP species present. The concentration of *trans*-2-pentene could not be increased further, because $[COP\text{-}Cl]_2$ was not soluble at greater concentrations of alkene. If the minor new peaks arise from palladium

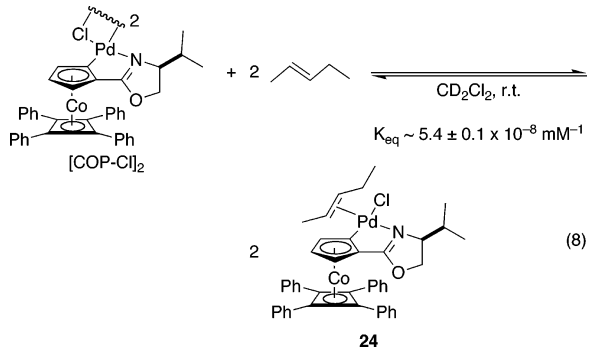

complex **24**, the equilibrium constant for palladium double-bond coordination is on the order of 10^{-8} mM^{-1}.

The binding of *Z* alkenes was also examined, using *cis*-2-hexene. The equilibrium constant of the reaction of $[COP\text{-}Cl]_2$ and this *cis*-alkene was much greater than that of the trans stereoisomer. Formation of a new COP complex could be observed by ^{1}H NMR spectroscopy, albeit as a mixture with $[COP\text{-}Cl]_2$ (eq 9).

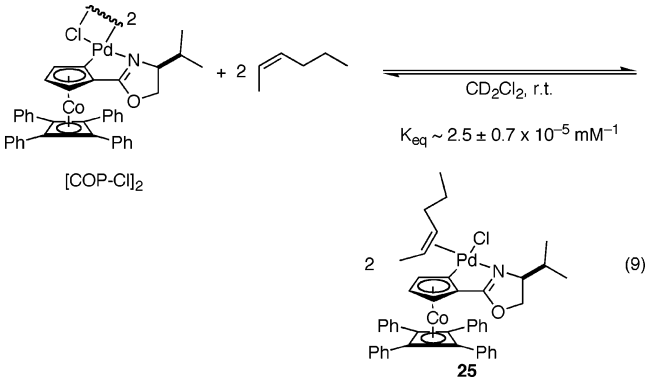

Because the binding affinity of trichloroacetimidate **22** is about 10^4 times greater than that of *trans*-2-pentene, the most likely structure of the catalyst−imidate complex is nitrogen-bound palladium species **21b**, not palladium−olefin complex **21a**.

2.3. Kinetic Simulation of $[COP\text{-}Cl]_2$-Catalyzed Allylic Trichloroacetimidate Rearrangement. To understand the possible role of nitrogen-bound palladium complex **21b** in the allylic trichloroacetimidate rearrangement, the mechanism shown in Scheme 5 was kinetically simulated.[22] With the use of three reactions differing in initial concentration of trichloroacetimidate **2a** and catalyst, the reaction rate constants were optimized to fit the observed concentrations of trichloroacetimidate **2a**, nitrogen-bound complex **21b**, and amide **3a**.[23] The rate constants shown in Scheme 5 were achieved by the following procedure. Initially, the rate constants for steps 1, 2, and 5 were defined as $k_1 = 10$ mM^{-2}·min^{-1}; $k_{-1} = 50\,000$ mM^{-1}·min^{-1}; $k_2 = 10$ mM^{-2}·min^{-1}; $k_{-2} = 2 \times 10^8$ mM^{-1}·min^{-1}; $k_5 = 500\,000$

(22) Gepasi, version 3.3, was employed in these simulations. See: (a) Mendes, P. *Comput. Appl. Biosci.* **1993**, *9*, 563−571. (b) Mendes, P. *Trends Biochem. Sci.* **1997**, *22*, 361−363. (c) Mendes, P.; Kell, D. B. *Bioinformatics* **1998**, *14*, 869−883.

(23) The initial concentrations chosen for imidate **2a**, nitrogen-bound palladium adduct **21b**, and amide **3a** for the three simulated reactions were as follows: For reaction 1, $[\mathbf{2a}]_0 = 530.3$ mM, $[\mathbf{21b}]_0 = 11.4$ mM, $[\mathbf{3a}]_0 = 3.2$ mM. For reaction 2, $[\mathbf{2a}]_0 = 565.6$ mM, $[\mathbf{21b}]_0 = 6.7$ mM, $[\mathbf{3a}]_0 = 0.9$ mM. For reaction 3, $[\mathbf{2a}]_0 = 553.8$ mM, $[\mathbf{21b}]_0 = 16.3$ mM, $[\mathbf{3a}]_0 = 0$ mM. The initial concentration of all other metabolites was defined to be 0 mM.

Scheme 5. Simulated Mechanism

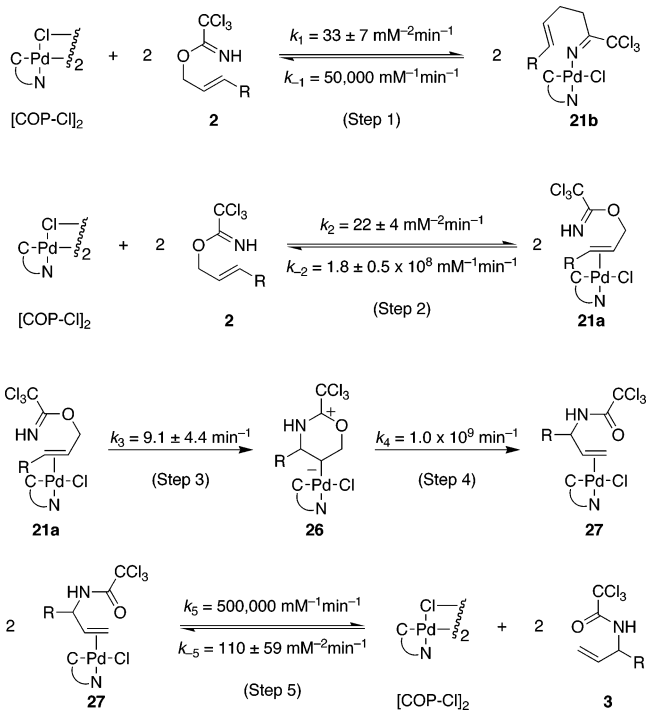

mM^{-1}·min^{-1}; k_{-5} = 10 mM^{-2}·min^{-1}. The absolute values of these rate constants were chosen randomly.[24] However, the ratio k_1/k_{-1} was chosen to mirror the equilibrium constant (K_{eq}) of the reaction of [COP-Cl]$_2$ and saturated imidate **22** (eq 7). The ratio k_2/k_{-2} reflects the equilibrium constant of the reaction of [COP-Cl]$_2$ and (*E*)-2-pentene (eq 8). The ratio k_5/k_{-5} was based on the equilibrium constant of the reaction of [COP-Cl]$_2$ and (*Z*)-2-hexene (eq 9), because the binding constant for terminal olefin **3** is probably more closely approximated by that of the less sterically encumbered *Z* olefin, rather than that of an *E* olefin. The value of k_3 was constrained to be less than k_4.[25] Then k_3 and k_4 were allowed to vary to optimize the fit to the experimentally observed concentrations. When no further improvement in fit was gained, the values of k_3 and k_4 were locked, while the values of k_1, k_{-1}, k_2, k_{-2}, k_5, and k_{-5} were allowed to vary. This process was repeated with the additional two experimental data sets. Good agreement was achieved between the observed and simulated data for all three species. The rate constants reported in Scheme 5 reflect the average values achieved by kinetic simulation of the three data sets.[26] The good fit between the simulated and experimental data shows that the mechanism illustrated in Scheme 5 is plausible for the allylic trichloroacetimidate rearrangement. These rate constants

Table 1. Enantioselectivity Provided by Various COP-Based Catalysts[a]

entry	imidate	R	catalyst (mol %)	%ee[b,c]
1	**2a**	CH_2CH_2Ph	[COP-Cl]$_2$ (5)	96
2	**2a**	CH_2CH_2Ph	[COP-Br]$_2$ (5)	96
3	**2a**	CH_2CH_2Ph	**28** (10)	97
4	**2a**	CH_2CH_2Ph	**5e** (10)[d]	97
5	**2a**	CH_2CH_2Ph	**29** (10)	96
6	**2b**	Me	[COP-Cl]$_2$ (5)	94
7	**2b**	Me	[COP-Br]$_2$ (5)	95
8	**2b**	Me	**28** (10)	95
9	**2b**	Me	**5e** (10)[d]	95[e]

[a] Conditions: imidate, catalyst, CH_2Cl_2 (0.6 M), 38 °C, 18 h. [b] Of the allylic trichloroacetamide product. Mean values from duplicate experiments (±1%), unless otherwise noted. [c] Determined by HPLC analysis. [d] 10 mol % excess tetrabutylammonium chloride was used in this reaction. [e] Determined by a single experiment.

and the simulated concentration of η^2-(alkene)palladium complex **21a** (>0.04 mM over the time course studied) also predict that the rate of C−N bond formation (step 3) is less than the rate of dissociation of intermediate **21a** (the reverse of step 2), suggesting that C−N bond formation is rate-determining in this mechanism.

Alternatively, palladium−olefin coordination (step 2, Scheme 5) could be irreversible. This mechanism was also evaluated using kinetic simulation. As before, the rate constants for steps 1 and 5 were initially set to ratios that corresponded to the equilibrium constants for the binding of the nitrogen atom of imidate **2a** and the binding of a terminal olefinic group, respectively.[27,28] The values for k_2, k_3, and k_4 were allowed to vary to optimize the fit to the experimentally observed concentrations of imidate **2a**, nitrogen-bound palladium adduct **21b**, and amide **3a**. Subsequently, the values of k_1, k_{-1}, k_5, and k_{-5} were allowed to vary while k_2, k_3, and k_4 were held constant. A variety of starting values for k_1, k_{-1}, k_5, and k_{-5} were examined to try to optimize the fit. While good agreement was achieved between the simulated and experimental data for [**2a**] and [**3a**] the concentration of nitrogen-bound palladium adduct **21b** was not fit well by the simulated data. Instead, the simulation predicted a more rapid decrease in [**21b**] than was experimentally observed. While we tested multiple initial guesses for k_1, k_{-1}, k_5, and k_{-5}, their absolute values are not known, making the simulation and the evaluation of this poor fit difficult. However, in light of the superior fit by the mechanism with reversible palladium double-bond coordination (discussed above), these simulations suggest that if formation of nitrogen-bound palladium complex **21b** is nonproductive, then palladium double-bond coordination is more likely reversible.

2.4. Dependence of Enantioselectivity on Ligands X and L. The effect of various neutral and anionic ligands on the enantioselectivity of the rearrangement of two allylic trichloroacetimidates was examined. No substantial change in enantioselectivity was observed in the rearrangement of allylic trichloroacetimidate **2a** or **2b** for any of the COP-based catalysts examined (Table 1). Little difference in enantiomeric excess was observed when [COP-Br]$_2$ was used instead of

(24) While we attained a good fit using these randomly chosen values, a good fit was also attained using different initial guesses for these rate constants, provided that the equilibria in steps 1, 2, and 5 were established rapidly compared to the rate of step 3. For example, an equally good fit was attained using the following initial values: k_1 = 0.1 mM^{-2}·min^{-1}; k_{-1} = 500 mM^{-1}·min^{-1}; k_2 = 0.1 mM^{-2}·min^{-1}; k_{-2} = 2 × 10^6 mM^{-1}·min^{-1}; k_5 = 5000 mM^{-1}·min^{-1}; k_{-5} = 0.1 mM^{-2}·min^{-1}. Similarly, a good fit was attained using these initial values: k_1 = 10 000 mM^{-2}·min^{-1}; k_{-1} = 50 000 000 mM^{-1}·min^{-1}; k_2 = 10 000 mM^{-2}·min^{-1}; k_{-2} = 2 × 10^{11}mM^{-1}·min^{-1}; k_5 = 5 × 10^8 mM^{-1}·min^{-1}; k_{-5} = 10 000 mM^{-2}·min^{-1}. Because a good fit does not depend on the absolute value of these rate constants, these kinetic simulations do not provide the absolute values of these constants.

(25) We assume that the fragmentation of alkylpalladium intermediate **26** is more facile than its formation. This assumption is supported by our computational studies below.

(26) The rate constants and graphs comparing the experimental and simulated data for each data set are included in the Supporting Information.

(27) The initial guesses for the absolute values of these rate constants (k_1, k_{-1}, k_5, and k_{-5}) were randomly made. However, none of our numerous initial guesses provided a good fit between the simulated and experimental concentration of nitrogen-bound palladium adduct **21b**.

(28) As before, we assume that the binding constant of the terminal olefinic group of amide **3a** is approximately equal to the binding constant of (*Z*)-2-hexene.

$[COP\text{-}Cl]_2$ (entries 1, 2, 6, and 7). No difference in enantioselectivity was observed between the benzoxazole-bound adducts of $[COP\text{-}Cl]_2$ and $[COP\text{-}Br]_2$ **28** and **29**, respectively (entries 3 and 5).[29,30] Finally, dichloropalladate **5e** also provided approximately the same enantioselectivity in the rearrangement of both trichloroacetimidates (entries 4 and 8). These similar enantioselectivities suggest that enantioinduction primarily stems from substrate interaction with the COP ligand.

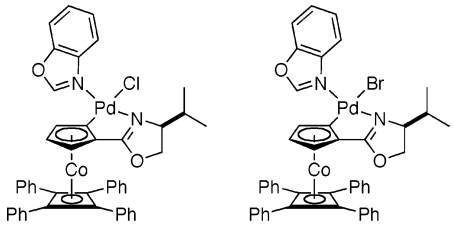

28 **29**

2.5. Computational Modeling. Because our kinetic studies suggested that palladium−olefin coordination is probably reversible, we turned to DFT calculations to model the probable rate- and enantiodetermining C−N bond formation step. The B3LYP/LACVP**+ level of theory[31] with "medium" or "fine" grid density as implemented in the Jaguar 5.5 quantum chemistry program package was utilized throughout this study.[32] For H, C, N, O, P, and Cl, the 6-31G basis set of Frisch et al. was used.[33] For cobalt, a Hay−Wadt small core effective potential replaces the 10 innermost core electrons.[34] For palladium, the 28 innermost core electrons are replaced by a Hay−Wadt small core effective potential.[34] The double asterisk (**) indicates the addition of polarization functions to atoms H through Ar. The single plus (+) indicates the addition of polarization functions to atoms Li through Ar. Full geometry optimization and analytical vibrational frequency calculation were performed on all models. Stationary points (intermediates) are characterized by exactly zero imaginary vibrations; transition-state structures are characterized by exactly one imaginary vibration. All energies are reported as electronic energies plus unscaled zero-point corrections. Free energies and enthalpies are reported in the Supporting Information. None of these calculations included solvent corrections.

2.5.1. $Pd(MeCN)_2Cl_2$-Catalyzed Rearrangement. Calculations of the cyclization-induced rearrangement mechanism were first performed on the $PdCl_2(MeCN)_2$-catalyzed allylic trichloroacetimidate rearrangement. $Pd(MeCN)_2Cl_2$ was selected because it is an efficient catalyst for the rearrangement of allylic trichloroacetimidates.[1] Additionally, its structure is much simpler than that of $[COP\text{-}Cl]_2$ and therefore facilitates efficient computations. In these computations, we assumed that acetonitrile, not chloride, dissociates upon coordination of the allylic imidate to form a neutral π-bonded palladium complex. The trichloromethyl group of the imidate was replaced with a hydrogen atom, and methyl was used as the R substituent on the double bond.

In this simplified system, the structure of the palladium−imidate adduct was computationally predicted to be intermediate **30** (Figure 5). In this structure, palladium is bound in an η^2 fashion to the double bond, which is positioned roughly perpendicular to the palladium square plane. This arrangement minimizes steric interactions between the imidate fragment and the other palladium ligands. The Pd−C distances are in agreement with those found in (η^2-alkene)palladium crystal structures.[35]

From this intermediate (**30**), calculations predict that C−N bond formation occurs through transition structure **31**, which is 8.9 kcal/mol higher in energy than intermediate **30** (Figure 5). In this transition structure, the allylic imidate fragment is in an envelope conformation with both the methyl substituent and the palladium atom in pseudoequatorial positions. The shorter C1−N and Pd−C2 distances evidence the formation of these bonds, coincident with the lengthening of the Pd−C1 distance (Table 2, entries 1 and 2). Frequency calculations on structure **31** revealed only one imaginary frequency, suggesting that it corresponds to a transition state. Also, intrinsic reaction coordinate calculations were used to confirm that transition-state structure **31** lies along the reaction coordinate of interest.[36]

The subsequent intermediate was computationally predicted to be the six-membered, cyclic structure **32** (Figure 5). A frequency calculation on structure **32** gave no imaginary frequencies, suggesting that it is indeed an intermediate. As in transition structure **31**, both ring substituents (palladium and methyl) are in pseudoequatorial positions, as predicted in the cyclization-induced rearrangement mechanism. In addition, the C1−C2 bond is positioned nearly perpendicular to the palladium square plane. The Pd−C1 distance (3.006 Å) is lengthened further than in transition structure **31** and is considerably longer than the Pd−C2 distance of 2.059 Å, confirming that this is not an η^2-(alkene)palladium species but rather an alkylpalladium complex with a σ-bond between Pd and C2 (Table 2, entries 2 and 3).[37] In comparison to the C1−N distance of 2.124 Å in transition structure **31**, the C1−N bond distance in intermediate **32** (1.509 Å) indicates formation of the nitrogen−carbon bond. This C−N bond distance is somewhat long, probably due to the partial sp^2 character of nitrogen.[38] This computed structure is in agreement with that predicted in the cyclization-induced rearrangement mechanism.

Fragmentation of intermediate **32** is predicted to proceed through transition structure **33** (Figure 5). This transition structure is calculated to be only 0.8 kcal/mol higher in energy than intermediate **33**, predicting that the Grob-like fragmentation

(29) Chloride **28** and bromide **29** were prepared by addition of benzoxazole to $[COP\text{-}Cl]_2$ and $[COP\text{-}Br]_2$, respectively. Their structures were confirmed by ^1H and ^{13}C NMR, IR, and mass spectroscopy as well as elemental analysis. In addition, X-ray crystallographic analysis of benzoxazole-bound palladium monomer **28** showed that benzoxazole is bound trans to the oxazoline ligand. See the Supporting Information for details.

(30) CCDC 626772 contains the supplementary crystallographic data for this paper. These data can be obtained free of charge from The Cambridge Crystallographic Data Centre via www.ccdc.cam.ac.uk/data_request/cif.

(31) For information on the B3LYP functional, see: (a) Becke, A. D. *J. Chem. Phys.* **1993**, *98*, 5648−5652. (b) Stephens, P. J.; Devlin, F. J.; Chabalowski, C. F.; Frisch, M. J. *J. Phys. Chem.* **1994**, *98*, 11623−11627. (c) Slater, J. C. *Quantum Theory of Molecules and Solids, Vol. 4: The Self-Consistent Field for Molecules and Solids*; McGraw-Hill: New York, 1974. (d) Becke, A. D. *Phys. Rev. A* **1988**, *38*, 3098−3100. (e) Vosko, S. H.; Wilk, L.; Nusair, M. *Can. J. Phys.* **1980**, *58*, 1200−1211. (f) Lee, C.; Yang, W.; Parr, R. G. *Phys. Rev. B* **1988**, *37*, 785−789. (g) Miehlich, B.; Savin, A.; Stoll, H.; Preuss, H. *Chem. Phys. Lett.* **1989**, *157*, 200−206.

(32) *Jaguar 5.5*, release 11; Schrödinger, L.L.C.: Portland, OR, 1991−2003.

(33) Frisch, M. J.; Pople, J. A.; Binkley, J. S. *J. Chem. Phys.* **1984**, *80*, 3265−3269.

(34) (a) Hay, P. J.; Wadt, W. R. *J. Chem. Phys.* **1985**, *82*, 270−283. (b) Hay, P. J.; Wadt, W. R. *J. Chem. Phys.* **1985**, *82*, 299−310.

(35) For an example of typical Pd−C distances in η^2-(alkene)palladium compounds, the four Pd−C distances in cyclooctadienylpalladium(II) chloride were determined to be 2.200, 2.209, 2.211, and 2.259 Å by X-ray crystallography. See: Rettig, M. F.; Wing, R. M.; Wiger, G. R. *J. Am. Chem. Soc.* **1981**, *103*, 2980−2986.

(36) See the Supporting Information for details.

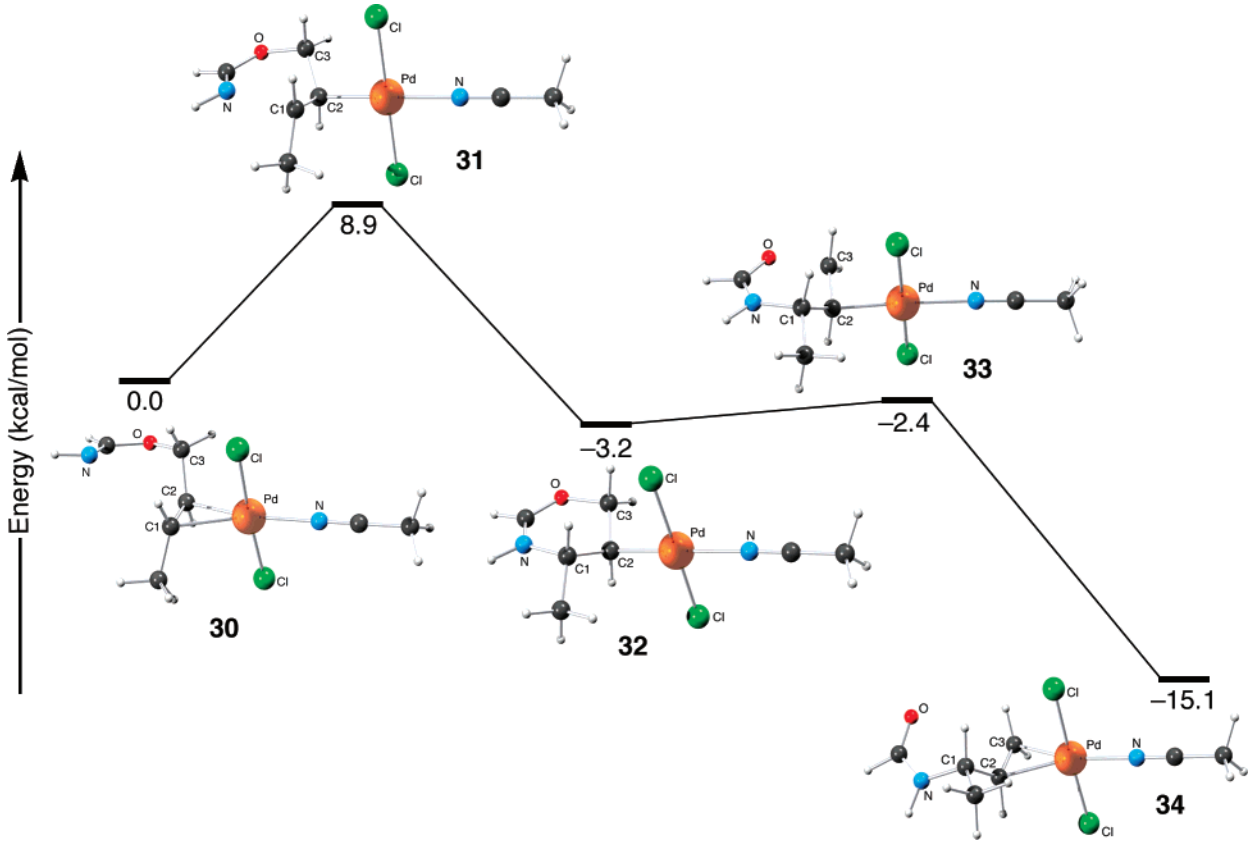

Figure 5. Computed structures and relative energies for the $Pd(MeCN)_2Cl_2$-catalyzed allylic imidate rearrangement.

Table 2. Selected Atom−Atom Distances in the Allylic Imidate Rearrangement

		distance (Å)				
entry	structure	Pd–C1	Pd–C2	Pd–C3	C1–N	C3–O
1	**30**	2.281	2.216	3.075	3.273	1.453
2	**31**	2.651	2.104	3.029	2.124	1.481
3	**32**	3.006	2.059	2.850	1.509	1.560
4	**33**	3.113	2.091	2.629	1.497	1.854
5	**34**	3.220	2.262	2.206	1.472	3.275

of intermediate **33** requires little energy. The carbon−oxygen bond cleavage is evidenced by lengthening of the C3−O distance with concurrent shortening of the Pd−C3 distance (Table 2, entry 4). Frequency calculations of structure **33** gave only one imaginary frequency, suggesting that this structure corresponds to a transition state. Also, intrinsic reaction coordinate calculations were used to confirm that transition-state structure **33** lies along the reaction coordinate of interest.[39]

The structure of the subsequent intermediate, the palladium−amide adduct, was computationally predicted to be π-complexed palladium intermediate **34** (Figure 5). As in intermediate **30**, palladium is bound in an η^2 fashion to the double bond, which is positioned roughly perpendicular to the palladium square plane, and the Pd−C distances are in agreement with those found in η^2-(alkene)palladium crystal structures.[40]

Comparison of the relative energies of structures **30**−**34** indicates that a cyclization-induced rearrangement mechanism via a six-membered, cyclic intermediate is reasonable for the palladium(II)-catalyzed allylic imidate rearrangement. The overall transformation of palladium-bound allylic imidate **30** to palladium-bound allylic amide **34** is predicted to be thermodynamically favored by 15.1 kcal/mol. This value closely matches the predicted energetic difference between a C═N bond and a C═O bond.[16] The energetic barrier for this transformation is predicted to be 8.9 kcal/mol, as shown by the relative energy of transition-state structure **31**. Because it most likely corresponds to the enantiodetermining step of the rearrangement, the six-membered, cyclic allylic imidate fragment of this transition-state structure was used as the initial guess for the imidate fragment in all subsequent transition-state calculations.

2.5.2. Coordination Geometry of Palladium in a COP Complex. In the $[COP\text{-}Cl]_2$-catalyzed rearrangement, the allylic imidate substrate can bind in one of two positions, either cis or trans to the oxazoline fragment.[29] To determine if there was an

(37) Bond lengths between palladium and an sp^3-hybridized carbon trans to an sp^2-hybridized nitrogen ligand can be 2.005−2.165 Å. For examples, see: (a) Newkome, G. R.; Gupta, V. K.; Taylor, H. C. R.; Fronczek, F. R. *Organometallics* **1984**, *3*, 1549−1554. (b) Kemmitt, R. D. W.; McKenna, P.; Russell, D. R.; Sherry, L. J. S. *J. Chem. Soc., Dalton Trans.* **1985**, 259−268. (c) Newkome, G. R.; Puckett, W. E.; Kiefer, G. E.; Gupta, V. K.; Fronczek, F. R.; Pantaleo, D. C.; McClure, G. L.; Simpson, J. B.; Deutsch, W. A. *Inorg. Chem.* **1985**, *24*, 811−826. (d) Newkome, G. R.; Kiefer, G. E.; Frere, Y. A.; Onishi, M.; Gupta, V. K.; Fronczek, F. R. *Organometallics* **1986**, *5*, 348−355. (e) Tempel, D. J.; Johnson, L. K.; Huff, R. L.; White, P. S.; Brookhart, M. *J. Am. Chem. Soc.* **2000**, *122*, 6686−6700. (f) Diversi, P.; Ingrosso, G.; Lucherini, A.; Lumini, T.; Marchetti, F.; Adovasio, V.; Nardelli, M. *J. Chem. Soc., Dalton Trans.* **1988**, 133−140. (g) Ruiz, J.; Martínez, T.; Rodríguez, V.; López, G.; Pérez, J.; Chaloner, P. A.; Hitchcock, P. B. *Dalton Trans.* **2004**, 3521−3527. (h) Schleis, T.; Heinemann, J.; Spaniol, T. P.; Mülhaupt, R.; Okuda, J. *Inorg. Chem. Commun.* **1998**, *1*, 431−434.

(38) Examples of C−N bond distances in simple molecules include 1.474, 1.462, and 1.451 Å. See: Dewar, M. J. S.; Thiel, W. *J. Am. Chem. Soc.* **1977**, *99*, 4907−4917.

(39) See the Supporting Information for details.

(40) For an example of typical Pd−C distances in η^2-(alkene)palladium compounds, the four Pd−C distances in cyclooctadienylpalladium(II) chloride were determined to be 2.200, 2.209, 2.211, and 2.259 Å by X-ray crystallography. See: Rettig, M. F.; Wing, R. M.; Wiger, G. R. *J. Am. Chem. Soc.* **1981**, *103*, 2980−2986.

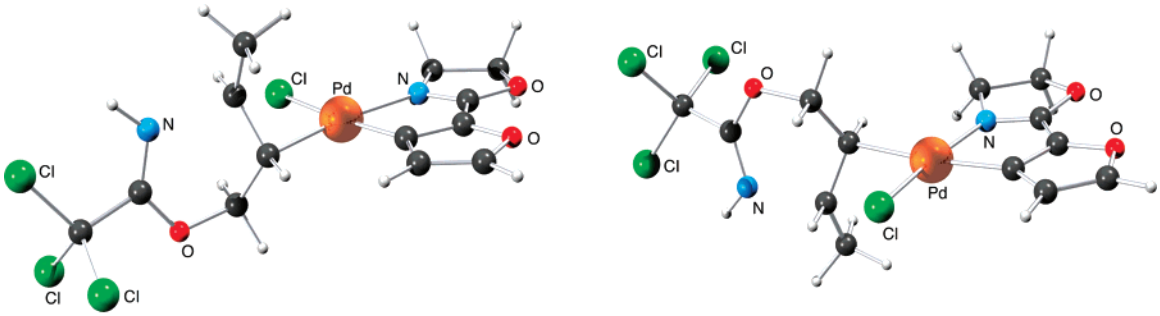

35

ΔE = 0 kcal/mol

36

ΔE = 6.9 kcal/mol

Figure 6. Relative energies of transition-state structures **35** and **36**.

electronic preference for one of these positions, 2-(2-furyl)-2-oxazoline was used as an electronic model for the ligand of $[COP\text{-}Cl]_2$. Natural bond order (NBO) analysis suggested that 2-(2-furyl)-2-oxazoline was a reasonable electronic model for the more complicated chiral ligand of $[COP\text{-}Cl]_2$.[39] Transition-state structures corresponding to C−N bond formation were calculated with the imidate fragment both cis and trans to the oxazoline. Several transition-state conformations were considered for both the cis and trans isomer, differing only in the dihedral angle about the C−Pd bond. Transition-state structure **35** was the lowest energy conformation with the alkyl fragment trans to the oxazoline (Figure 6). The lowest energy conformation with the alkyl fragment cis to oxazoline was transition-state structure **36**. As shown, trans-oriented transition-state structure **35** is significantly lower in energy than cis-oriented transition-state structure **36**. For the COP ligand, the isopropyl oxazoline substituent probably further disfavors imidate coordination cis to the oxazoline fragment due to greater steric hindrance.

2.6. The $[COP\text{-}Cl]_2$-Catalyzed Rearrangement. On the basis of the transition-state structure calculations of these simpler systems, transition-state conformations corresponding to the enantiodetermining step of the $[COP\text{-}Cl]_2$-catalyzed allylic trichloroacetimidate rearrangement were calculated. For these calculations, the ligand geometry of the X-ray crystal structure of benzoxazole-bound palladium monomer **28** was used as the initial guess for the COP ligand.[29] The isopropyl group of the COP ligand was simplified to methyl. The geometry of the allylic imidate fragment in structure **31** was used as the initial guess for the allylic imidate geometry. As shown in Scheme 6, four transition-state structures were found with the imidate coordinated trans to the oxazoline fragment. No transition-state structures could be found with the imidate bound cis to the oxazoline. In all four trans-oriented transition-state structures, the allylic imidate fragment is in an envelope conformation with both the methyl substituent and palladium in pseudoequatorial positions. In all four computed structures, the N2−C39 distance is calculated to be between 2.027 and 2.096 Å. This distance is similar to that predicted in the $PdCl_2(MeCN)_2$ system. Frequency calculations of these four structures showed that the major component of the transition vector consists of a shortening of the N2−C39 distance. Nitrogen attack on the *Si* olefin face in structures **37** and **38** leads to major observed enantiomer (*S*)-**41**, whereas N2−C39 bond formation in structures **39** and **40** provides the minor observed enantiomer.[41] The primary difference between structures **37** and **38** is rotation around the Pd−C bond. In structure **37**, the allylic imidate is oriented with the methyl substituent away from the tetraphenylcyclobutadienyl fragment of the ligand, whereas the imidate methyl group is oriented toward the tetraphenylcyclobutadienyl fragment in structure **38**. Rotation around the Pd−C bond also distinguishes structures **39** and **40**. The lowest energy calculated transition-state structure **37** correctly predicts the sense of enantioinduction. In light of the small energy differences that are observed between these diastereomeric transition structures, the significance of these computational conclusions is unclear. Nonetheless, in the context of providing models for identifying potentially important steric interactions and predicting possible profitable modifications of catalyst architecture, we find that these calculations provide useful guidance.

In all four structures, the allylic imidate fragment appears to be positioned to minimize steric interactions with the ligands directly coordinated to palladium. For example, in structure **37**, the imidate fragment is positioned so that H38 eclipses the Pd−Cp bond. This arrangement minimizes steric interactions between the chloride ligand and either C39 or C41. Alternatively, when the alkyl fragment is rotated as in conformation **38**, an eclipsed arrangement of H38 and the chloride allows C39 and C41 to be gauche to the Pd−Cp bond. In structures **39** and **40**, similar interactions are observed.

Although the conformations of structures **38** and **39** minimize the steric interaction between the cyclopentadienyl ring and C41 of the allylic imidate, these groups are still quite close, as shown by the proximity of their closest hydrogen atoms (Table 3). In structure **38**, the H32−H6 distance is only 2.150 Å, whereas the H38−H6 distance is 2.259 Å in structure **37** (entries 1 and 2). Similarly, the distance between H32 and H6 is 2.143 Å in transition-state structure **39**, whereas the H38−H6 distance is longer in structure **40** (entries 3 and 4). Because structures **38** and **39** are predicted to be highest in energy, avoidance of steric interactions between the imidate fragment and the cyclopentadienyl ring seems to be a major factor in determining transition-state conformation.

Another potentially important interaction is between the allylic imidate fragment and the tetraphenylcyclobutadienyl fragment of the chiral ligand. As shown in Table 4, conformations **38**

(41) From the preceding π-complexed palladium intermediates, the activation energies for these transition states were calculated to be 11.9 kcal/mol for transition structure **37**, 16.3 kcal/mol for transition structure **38**, 16.4 kcal/mol for transition structure **39**, and 11.5 kcal/mol for transition structure **40**.

Scheme 6. Enantiodetermining Transition-State Structures

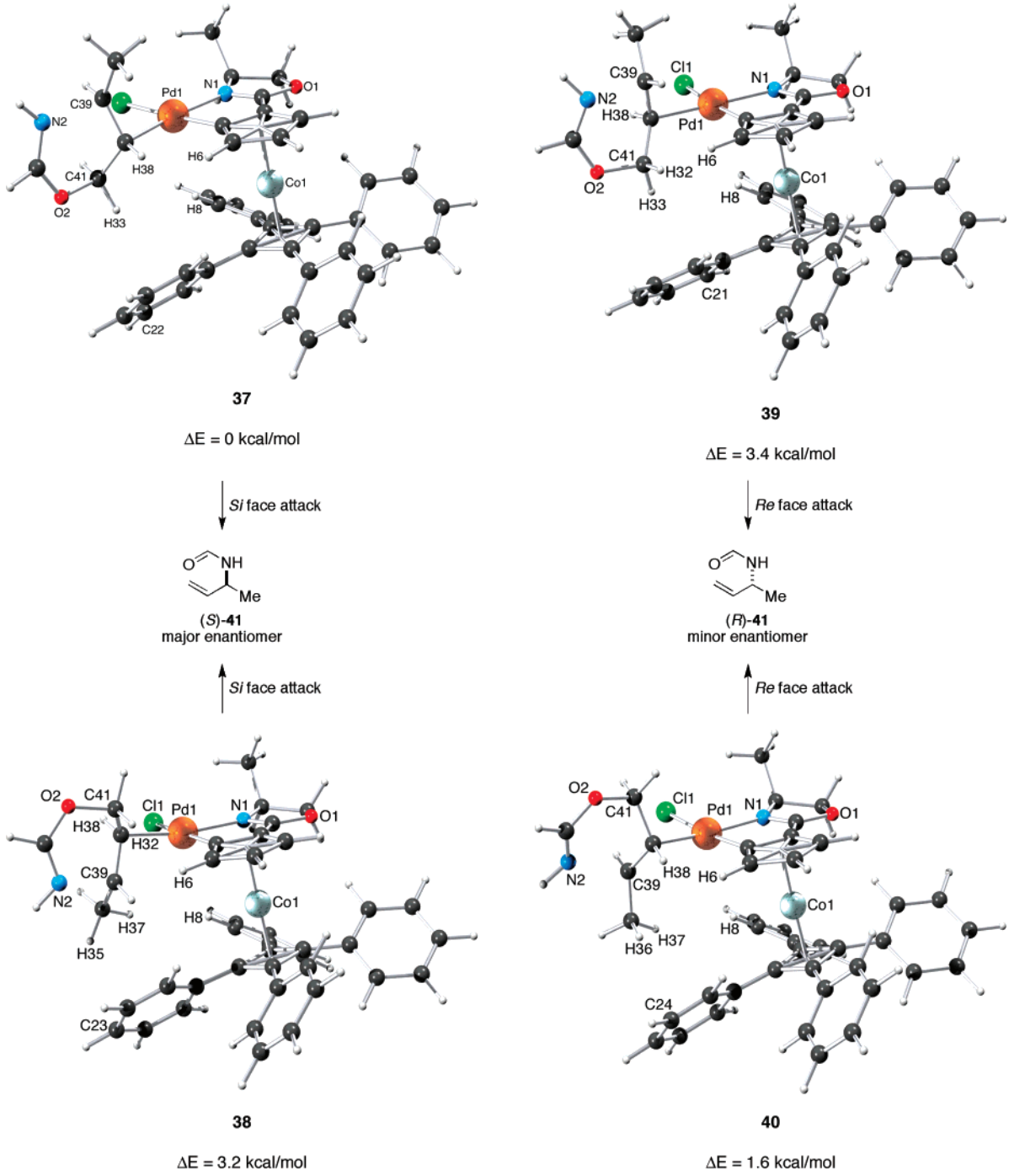

Table 3. Closest Contacts between the Allylic Imidate Fragment and the Cyclopentadienyl Ring

		ΔE	H–H distance	
entry	structure	(kcal/mol)	atoms	distance (Å)
1	**37**	0	H38−H6	2.259
2	**38**	3.2	H32−H6	2.150
3	**39**	3.4	H32−H6	2.143
4	**40**	1.6	H38−H6	2.245

Table 4. Closest Contacts between the Imidate Fragment and Tetraphenylcyclobutadienyl Fragment

		ΔE	H–H distance		H–C distance	
entry	structure	(kcal/mol)	atoms	distance (Å)	atoms	distance (Å)
1	**37**	0	H33−H8	3.036	H33−C22	3.100
2	**38**	3.2	H37−H8	2.595	H35−C23	3.126
3	**39**	3.4	H33−H8	3.225	H33−C21	3.096
4	**40**	1.6	H37−H8	2.665	H36−C24	2.913

and **40**, which position the imidate methyl substituent near the tetraphenylcyclobutadienyl floor, suffer closer contact between the hydrogen atoms of the imidate methyl group and those of the phenyl rings. However, these H−H closest contacts do not parallel the relative energies of the structures. A comparison of the closest hydrogen−carbon distances shows that these closest contacts are all about 3.1 Å in conformations **37**, **38**, and **39** (entries 1−3). In contrast, this distance is only 2.913 Å in transition-state structure **40**, suggesting that structure **40** may be destabilized by this interaction (entry 4).

Scheme 7. Intramolecular Formation of Palladium−Olefin Complex **21a** via **21b**

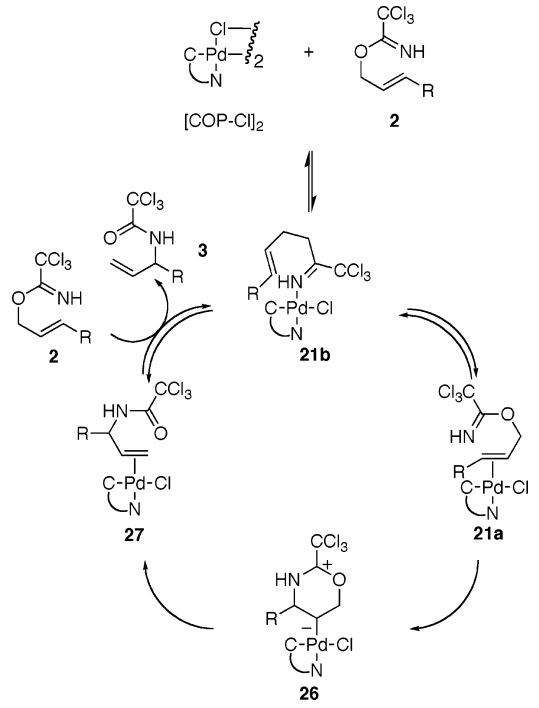

Discussion

A Nitrogen-Bound Catalyst−Imidate Complex and Reversibility of Olefin−Palladium Coordination. Our kinetic studies of the palladium(II)-catalyzed allylic trichloroacetimidate rearrangement support reversible formation of a nitrogen-bound imidate−catalyst adduct. The rearrangement catalyzed by dichloropalladate **5e** showed rate inhibition by excess chloride, suggesting that reversible dissociation of one chloride ligand from dichloropalladate **5e** occurs before the rate-determining step. Furthermore, the observation of saturation kinetics when $[COP\text{-}Cl]_2$ was used as catalyst also indicates reversible formation of a catalyst−imidate complex. The relative binding constants for saturated trichloroacetimidate **22** (2.2×10^{-4} mM^{-1}) and *trans*-2-pentene (5.4×10^{-8} mM^{-1}) suggest that the identity of this catalyst−imidate complex is nitrogen-bound palladium species **21b**, not η^2-(alkene)palladium complex **21a**.

The role of nitrogen-bound adduct **21b** in the allylic trichloroacetimidate rearrangement mechanism is somewhat unclear. Even though the catalyst resting state under saturation conditions may be nitrogen-bound species **21b**, the $[COP\text{-}Cl]_2$-catalyzed allylic trichloroacetimidate rearrangement most likely proceeds through transient η^2-(alkene)palladium adduct **21a**. In analogy to the $PdCl_2(MeCN)_2$-catalyzed rearrangement, the $[COP\text{-}Cl]_2$-catalyzed rearrangement fails to proceed if there is a substituent at C2 of the allylic trichloroacetimidate.[1,42] This fact supports a cyclization-induced mechanism in which olefin rather than nitrogen coordinates to palladium, activating the double bond toward nucleophilic attack. Formation of nitrogen-bound adduct **21b** may then be either a nonproductive reversible binding event, which does not lie on the catalytic cycle (Scheme 5), or a productive step leading to formation of η^2-(alkene)palladium intermediate **21a** (Scheme 7). These two mechanistic possibilities cannot be distinguished by our kinetic data.

We investigated whether olefin−palladium coordination was reversible by numerically fitting our kinetic data to both the nonproductive nitrogen-binding mechanism (Scheme 5) and the productive nitrogen-binding mechanism (Scheme 7). In the case of nonproductive formation of nitrogen adduct **21b**, the experimental data were fit well by a mechanism in which formation of η^2-(alkene)palladium adduct **21a** was reversible. A mechanism involving irreversible palladium−olefin coordination was less well fit by the experimental data. However, the kinetic data were well fit by a mechanism in which nitrogen-bound adduct **21b** productively undergoes intramolecular rearrangement to η^2-(alkene)palladium adduct **21a**. In this case, the kinetic simulation provided good fits for both reversible and irreversible palladium−olefin coordination. Because we cannot rigorously exclude the possibility of intramolecular rearrangement of nitrogen-bound adduct **21b** to η^2-(alkene)palladium intermediate **21a**, the possibility that palladium−olefin coordination is irreversible cannot be disqualified. However, as suggested by Hollis and Overman, the rate- and enantiodetermining step of the nonasymmetric palladium(II)-catalyzed rearrangement of trichloroacetimidates seems to be nucleophilic attack of nitrogen at the activated olefin (see the Introduction). This hypothesis requires that palladium−olefin coordination must be reversible.

Rate- and Enantiodetermining Step. The DFT calculations carried out during this study lend further support for a cyclization-induced rearrangement mechanism, in which C−N bond formation is the rate- and enantiodetermining step. First, DFT calculations using $PdCl_2(MeCN)_2$ as a model catalyst suggest that the cyclization-induced rearrangement is an energetically accessible pathway for this reaction. As originally hypothesized in the cyclization-induced rearrangement mechanism,[5] attack of the imidate nitrogen at the activated alkenyl group yields a six-membered, cyclic alkylpalladium intermediate. This alkylpalladium intermediate then fragments to give the palladium-bound amide. Calculations predict that alkylpalladium intermediate **32** has no imaginary frequencies and sits in a shallow energy well; therefore, it does not appear to be a transition-state structure but rather a discrete intermediate in this reaction. The computational analysis, coupled with the kinetic experiments and previous observations of the palladium(II)-catalyzed allylic trichloroacetimidate rearrangement, provides convincing support for C−N bond formation being the rate- and enantiodetermining step of the allylic trichloroacetimidate rearrangement.

Rate-determining formation of the C−N bond through an envelope, six-membered cyclic transition state offers an explanation for the rate difference between the rearrangements of allylic trichloroacetimidates with *E* vs *Z* olefin configuration. Whereas the rearrangement of (*E*)-olefin **2c** proceeded in 99% yield and 95% ee, (*Z*)-olefin **2d** gave only 17% yield of amide **3d** (71% ee) after the same reaction time (eq 10).[2a] For allylic

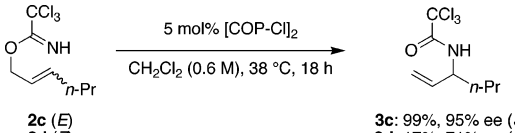

(10)

trichloroacetimidates with *E* olefin geometry, pseudoequatorial orientation of both R and palladium is possible in the favored six-membered cyclic transition state (**42**, Figure 7). In contrast,

(42) Anderson, C. E. Ph.D. Dissertation, University of California, Irvine, CA, 2003.

42 (from *E*-olefin) **43** (from *Z*-olefin)

Figure 7. Conformations of cyclic transition-state structures from *E* and *Z* olefins.

the rearrangements of allylic trichloroacetimidates with *Z* olefin geometry might be slower, because they proceed through either an envelope conformation with R or palladium pseudoaxial (**43**) or a higher-energy boatlike conformation. These relative rearrangement rates are consistent with nitrogen attack on the activated olefin being the rate-determining step in the cyclization-induced mechanism.

In contrast, in the $[COP\text{-}OCOCF_3]_2$-catalyzed rearrangement of more electron-rich allylic *N*-(*p*-methoxyphenyl)benzimidates, the reaction is faster and more selective with *Z* allylic trichloroacetimidates than with their *E* stereoisomers.[12,43] The fact that the opposite trend is observed with benzimidates is consistent with the rate of nucleophilic attack by the imidate nitrogen on the activated double bond being faster with these electron-rich benzimidates, perhaps causing palladium−olefin coordination to be rate-determining.

A Model for Stereoinduction. Our computational studies predict that the more favorable transition-state structure has the allylic imidate trans to the oxazoline fragment of the chiral ligand. When 2-(2-furyl)-2-oxazoline was employed as an electronic model for the chiral ligand of $[COP\text{-}Cl]_2$, transition-state configuration **35** with a trans relationship between the imidate and oxazoline fragments was favored over the cis-configured **36** by almost 7 kcal/mol (Figure 6). These relative energies can be understood in terms of the trans effect; in transition structure **35** the π-accepting chloride ligand is trans to the strongest π-donor, the cyclopentadienyl ring, whereas the allylic imidate substituent trans to the oxazoline nitrogen is essentially an alkyl substituent.[44] Because the oxazoline fragment of $[COP\text{-}Cl]_2$ is more sterically encumbered by the isopropyl group, we expect that the energy difference between these configurations will be even more significant with COP catalysts. Our inability to locate transition-state structures with the alkyl fragment cis to the oxazoline in the COP system suggests that these transition states, if they exist, are higher in energy than those with the alkyl fragment trans to the oxazoline. This trans configuration places the allylic imidate fragment far away from the isopropyl substituent on the oxazoline ring, suggesting that changing the oxazoline substituent will have little effect on the enantioselectivity of the rearrangement; thus, the planar chirality of the COP ligand is largely responsible for the observed enantioselectivity.

The importance of the ligand's planar chirality is evidenced in the calculated transition-state structures, which allow the development of a model for the enantioselectivity observed in the $[COP\text{-}Cl]_2$-catalyzed allylic trichloroacetimidate rearrangement. The relative energies of the calculated transition-state

Scheme 8. Model for Enantioinduction

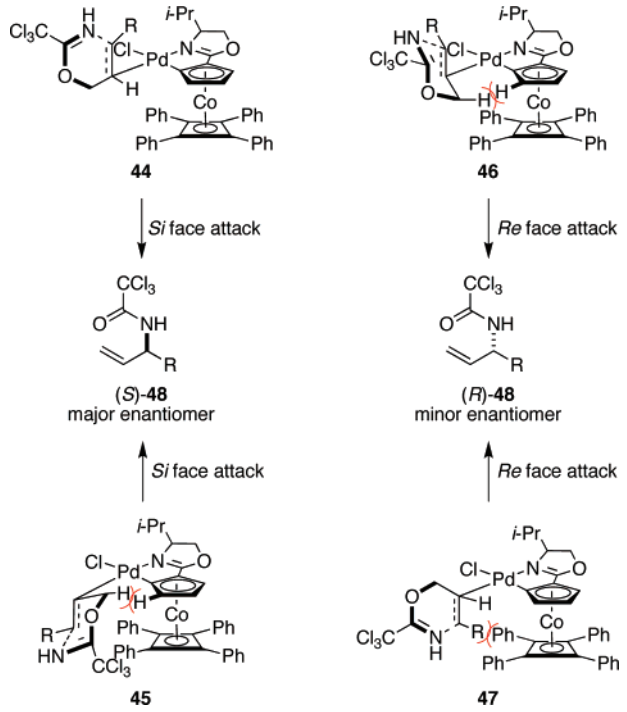

structures for the enantiodetermining step correctly predict that formation of enantiomer (*S*)-**41** will be favored.[45] Comparison of the four transition-state structures suggests that minimization of steric interactions between the imidate fragment and the cyclopentadienyl ring is a major factor influencing their stability. As illustrated schematically in Scheme 8, significant steric interactions develop between the Cp-H and the imidate methylene in conformations **45** and **46**, which correspond to the highest energy transition-state conformations. Interaction with the cyclopentadienyl ring is minimized in structures **44** and **47**, in which the allylic methylene is positioned away from the cyclopentadienyl ring.

Comparison of the two lower-energy transition-state structures (**44** and **47**) suggests that steric hindrance between the trichloroacetimidate R substituent and the tetraphenylcyclobutadiene floor destabilizes conformation **47**. Thus, conformation **44**, which lacks this destabilizing interaction, is the favored transition-state structure. This analysis explains why allylic trichloroacetimidates with larger R substituents rearrange with higher enantioselectivity; conformation **47** would be even more disfavored by a larger R group interacting with the tetraphenylcyclobutadiene fragment.

The model for enantioinduction we have developed suggests a way to rationally design more enantioselective COP-based catalysts. If the observed enantioselectivity in the $[COP\text{-}Cl]_2$-catalyzed allylic trichloroacetimidate rearrangement is a result of the energy difference between structures **44** and **47** (Scheme 8), further destabilization of transition structure **47** should lead to greater enantioselectivity. Destabilization of structure **47** should be achieved by increasing the steric bulk of the

(43) As with $[COP\text{-}Cl]_2$, the $[COP\text{-}OCOCF_3]_2$-catalyzed rearrangement of electron-poor *N*-(*p*-methoxyphenyl)trifluoroacetimidates proceeds more quickly for *E* olefins than for *Z*. See ref 4i. In contrasting the reactivity of trifluoroacetimidates and benzimidates, then, the difference in relative rearrangement rates of *E* vs *Z* olefins most likely arises from differing nucleophilicity of the imidate nitrogen.

(44) Hartley, F. R. *Chem. Soc. Rev.* **1973**, *2*, 163−179.

(45) The magnitude of the energy difference between calculated transition-state structures **37** and **40** is 1.6 kcal/mol. This value is in close agreement to the $\Delta\Delta G^{\ddagger}$ measured by the experimentally determined enantiomeric ratio (2.0 kcal/mol at 298 K). Because the entropy of these transition-state structures should be similar, the electronic energies plus zero-point corrections should correlate with the relative Gibbs free energies.

tetraarylcyclobutadiene floor. The modular nature of the [COP-Cl]$_2$ synthesis allows facile introduction of bulkier aryl groups to this portion of the catalyst for testing of this hypothesis.[46,47]

Conclusions

The data acquired during this study is consistent with a cyclization-induced mechanism for the [COP-Cl]$_2$-catalyzed rearrangement of allylic trichloroacetimidates. Formation of the palladium−olefin intermediate may occur either intermolecularly by association of the double bond of free allylic trichloroacetimidate to palladium or intramolecularly by rearrangement of the nitrogen-bound palladium−imidate complex **21b**. The possibility that palladium−olefin coordination is irreversible and therefore rate-limiting seems unlikely based on our kinetic studies, kinetic simulations, and the relative rearrangement rates of *E* and *Z* allylic trichloroacetimidates. The rate- and enantiodetermining step is more likely C−N bond formation. Computational studies support the intermediacy of a six-membered, cyclic alkylpalladium species, which was originally hypothesized in the cyclization-induced rearrangement mechanism.

Calculations were also used to develop a model for enantioinduction in the [COP-Cl]$_2$-catalyzed rearrangement of allylic trichloroacetimidates. Several features of this model are worth noting. First, the planar chirality of the COP ligand, rather than the chirality in the oxazoline ring, imparts enantioselectivity in this reaction.[48] The favored conformation of the transition-state structure corresponding to the enantiodetermining step has the allylic imidate fragment coordinated trans to the oxazoline fragment, far from the oxazoline stereocenter. Second, comparison of the possible conformations of this transition-state structure suggests that two factors cooperate to provide the observed enantioselectivity. Steric interactions between the allylic imidate and the cyclopentadienyl ring of the COP ligand destabilize two of the four possible conformations. In addition, steric hindrance from the tetraphenylcyclobutadiene fragment of the COP ligand contributes to the observed enantioselectivity by destabilizing the transition state leading to the minor enantiomer of product.

This model for enantioinduction predicts that the framework of [COP-Cl]$_2$ can be rationally improved to increase the enantioselectivity of the allylic trichloroacetimidate rearrangement. Optimization of the catalyst should focus on varying the aryl rings of the tetraarylcyclobutadiene floor and on substitution of the cyclopentadienyl fragment. Changes in the steric bulk of the oxazoline substituent are not expected to affect the enantioselectivity. Current research efforts in the Overman laboratories are directed toward exploring these predictions.

Experimental Section

In Situ Generation of Dichloropalladate 5e. In a glovebox, [COP-Cl]$_2$ (8.8 mg, 0.0060 mmol) was weighed into a 1 mL volumetric flask. A solution of tetrabutylammonium chloride (6.7 mg, 0.024 mmol) and CD_2Cl_2 was added to the volumetric flask. The total volume was brought to 1 mL by the addition of more CD_2Cl_2. A portion of this solution was then transferred to an NMR tube. Dichloropalladate **5e** thus formed was characterized as a 1:1 mixture with excess Bu_4NCl: ^{1}H NMR (400 MHz, CD_2Cl_2) δ 7.59−7.62 (m, 8H), 7.19−7.23 (m, 12H), 5.1 (app d, 1H), 4.6 (app d, 1H), 4.2 (t, J = 2.4 Hz, 1H), 4.1 (dd, J = 3.8, 8.2 Hz, 1H), 3.2−3.3 (m, 10H of **5e** + 8H of Bu_4NCl), 2.6 (m, 1H), 1.63 (qn, J = 8.0 Hz, 8H of **5e** + 8H of Bu_4NCl), 1.41 (h, J = 7.4 Hz, 8H of **5e** + 8H of Bu_4NCl), 1.0 (t, J = 7.4 Hz, 12H of **5e** + 12H of Bu_4NCl), 0.73 (d, J = 7.2 Hz, 3H), 0.64 (d, J = 6.8 Hz, 3H); ^{13}C (100 MHz, CD_2Cl_2) δ 170.7, 136.1, 129.5, 128.1, 126.0, 100.2, 86.5, 85.6, 84.9, 80.4, 75.9, 71.2, 66.1, 59.2, 28.7, 24.4, 20.0, 18.7, 14.0, 13.7. Detection of the dichloropalladate anion by mass spectroscopy was hindered, because the mass spectrum was saturated by peaks corresponding to $(Bu_4N)_nCl_{(n+1)}$.[49] However, the mass spectrum of a solution of [COP-Cl]$_2$ and CsCl in CH_2Cl_2 displayed a peak corresponding to the mass of the dichloropalladate anion: LRMS (ESI) *m*/*z* 768 [766 calcd for $C_{39}H_{33}Cl_2CoNOPd$ (M)].

General Procedure for Kinetic Experiments Using Catalyst 5e. In a glovebox, stock solutions of trichloroacetimidate **2a**, [COP-Cl]$_2$, tetrabutylammonium chloride, and 1,3,5-trimethoxybenzene were combined in a 1 mL volumetric flask. Then CD_2Cl_2 was added to bring the total volume to 1 mL. A portion of this solution was transferred to an NMR tube, which was fitted with a Cajon adapter, removed from the glovebox, and sealed under reduced pressure. After obtaining an initial ^{1}H NMR spectrum (t = 0), the NMR tube was submerged in a preheated oil bath at 60 ± 1 °C. The reaction progress was monitored by ^{1}H NMR.

General Procedure A for Kinetic Studies of the [COP-Cl]$_2$-Catalyzed Allylic Trichloroacetimidate Rearrangement: Determination of the Kinetic Order of Trichloroacetimidate 2a. In a nitrogen atmosphere glovebox, 0.1 mL of a stock solution of [COP-Cl]$_2$ (0.024 M), 1,3,5-trimethoxybenzene (0.12 M), and CD_2Cl_2 was transferred to an NMR tube, which was fitted with a Cajon and removed from the glovebox. After the [COP-Cl]$_2$ solution was frozen using liquid N_2, a solution of imidate **2a** and CD_2Cl_2 (0.3 mL) was added to the NMR tube under a nitrogen atmosphere. The NMR tube was then sealed under reduced pressure. The resulting solution was kept between −78 and 0 °C until immediately before injection into the NMR probe, which was preheated to 310 ± 1 K. ^{1}H NMR spectra were acquired every 3−5 min.

General Procedure B for Kinetic Studies of the [COP-Cl]$_2$-Catalyzed Allylic Trichloroacetimidate Rearrangement: Determination of the Kinetic Order of Catalyst 21. In a nitrogen atmosphere glovebox, 0.3 mL of a stock solution of trichloroacetimidate **2a** (2.4 M), 1,3,5-trimethoxybenzene (0.079 M), and CD_2Cl_2 was transferred to an NMR tube, which was fitted with a Cajon and removed from the glovebox. After the imidate solution was frozen using liquid N_2, a solution of [COP-Cl]$_2$ and CD_2Cl_2 (0.3 mL) was added to the NMR tube under a nitrogen atmosphere. The NMR tube was then sealed under reduced pressure. The resulting solution was kept between −78 and 0 °C until immediately before injection into the NMR probe, which was preheated to 310 ± 1 K. ^{1}H NMR spectra were acquired every 3−5 min.

(46) (a) Anderson, C. E.; Overman, L. E.; Richards, C. J.; Watson, M. P.; White, N. *Org. Synth.* **2007**, *84*, 139−147. (b) Anderson, C. E.; Kirsch, S. F.; Overman, L. E.; Richards, C. J.; Watson, M. P. *Org. Synth.* **2007**, *84*, 148−155.

(47) In addition to improving COP-based catalysts, this mechanistic model may also account for recently reported results (see ref 13). The Peters group tested a variety of ferrocenium−imidazoline palladacycles in the rearrangement of allylic *N*-(*p*-methoxyphenyl)trifluoroacetimidates. Whereas varying the imidazoline substituents had little effect on the enantioselectivity, increasing the size of the substituent on the terminal cyclopentadienyl ring led to substantially improved enantioselectivity. Our model for enantioinduction is consistent with these results. In the enantiodetermining step, the allylic trifluoroacetimidate fragment is bound trans to the imidazolinyl fragment. Enantioselectivity arises because the transition-state structure leading to the minor enantiomer is disfavored by steric hindrance between the C3-substituent of the allylic imidate fragment and the C_5R_5 fragment of the catalyst. This explanation assumes that the rate-determining step of the rearrangement of allylic *N*-(*p*-methoxyphenyl)trifluoroacetimidates is C−N bond formation. This assumption seems valid, because the relative rearrangement rates of allylic *N*-(*p*-methoxyphenyl)trifluoroacetimidates with *E* vs *Z* olefin geometries mirror those of allylic trichloroacetimidates.

(48) The importance of the planar chirality of COP catalysts has been previously investigated. See: Prasad, R. S.; Anderson, C. E.; Richards, C. J.; Overman, L. E. *Organometallics* **2005**, *24*, 77−81.

(49) The only peaks seen in the mass spectrum correspond to $(Bu_4N)_nCl_{(n+1)}$ ions.

In Situ Generation of Imidate−Palladium Complex 23. In a nitrogen atmosphere glovebox, $[COP\text{-}Cl]_2$ (0.016 mmol, 24 mg), trichloroacetimidate **22** (0.85 mmol, 150 mg), and CD_2Cl_2 (0.4 mL) were combined in an NMR tube, which was fitted with a Cajon and removed from the glovebox. The NMR tube was then sealed under reduced atmosphere. The resulting solution of complex **23** and excess imidate **22** was analyzed by NMR spectroscopy. With the use of a combination of ^1H, DOSY, HMQC, and HMBC experiments, the following ^1H and ^{13}C NMR peaks corresponding to complex **23** were assigned: ^1H NMR (500 MHz, CD_2Cl_2) δ 7.65 (s, 1H, N*H*), 4.85 (s, 3H, OCH_3), 4.73 (d, $J = 2.0$ Hz, 1H, Cp*H*), 4.63 (t, $J = 2.5$ Hz, 1H, Cp*H*), 4.54 (br, 1H, Cp*H*), 4.30 (d, $J = 4.0$ Hz, 1H, CH_2), 3.53 (m, 2H, C*H*, CH_2), 2.68 (m, 1H, C*H*), 0.80 (d, $J = 7.0$ Hz, 3H, CH_3), 0.70 (d, $J = 7.0$ Hz, 3H, CH_3); ^{13}C NMR (125 MHz, CD_2Cl_2) δ 172.3, 166.2 (imidate C═N), 134.9, 128.8, 127.3, 100.3, 90.0 (imidate *C*Cl_3), 85.8, 85.5, 83.6, 79.8, 75.7, 71.4, 65.6, 60.8 (imidate *C*H_3), 28.7, 18.3, 13.6. HRMS (ESI) *m*/*z* 873.0300 (873.0283 calcd for $C_{42}H_{37}Cl_3CoN_2O_2Pd$ (M − Cl).

General Procedure for Rearrangement of Allylic Trichloroacetimidates Using Various COP-Based Catalysts (Table 1). A solution of catalyst (0.008 mmol or 0.016 mmol, as noted in Table 1) and CH_2Cl_2 (0.26 mL) was added to trichloroacetimidate **2** (0.16 mmol) in an oven-dried, 1 dram vial. The vial was capped and then maintained at 38 °C. After 18 h, the solution was concentrated. Purification by silica gel column chromatography provided allylic trichloroacetamide **3**. Chiral HPLC analysis (Chiralpak AS, 99:1 *n*-hexane/IPA, 1.0 mL/min) was used to determine the enantiomeric excess of **3a**. Chiral HPLC analysis (Whelk-O 1, 99:1 *n*-hexane/IPA, 1.0 mL/min) was used to determine the enantiomeric excess of **3b**.

Acknowledgment. This research was supported by NSF (CHE-9726471) and a predoctoral fellowship for M.P.W. from Allergan, Inc. Additional unrestricted support from Amgen, Roche Palo Alto, Merck, and Pfizer is gratefully acknowledged. NMR spectra were determined at U.C. Berkeley, using instruments acquired with the assistance of NSF and NIH shared instrumentation grants. We thank Dr. Herman van Halbeek for his assistance with several NMR experiments. Mass spectra were determined at U.C. Irvine using instruments acquired with the assistance of NSF and NIH shared instrumentation grants. Dr. John Greaves is acknowledged for his assistance with obtaining several mass spectra. DFT calculations were performed by M.P.W. at the U.C. Berkeley Molecular Graphics Facility. We thank Dr. Kathleen Durkin and Jamin Krinsky for helpful computational discussions.

Supporting Information Available: General methods, experimental procedures for the preparation of palladium compounds **5e**, **28**, and **29**, additional kinetic data, kinetic simulation data, computational data, NMR and HPLC spectra, CIF file for compound **28**. This material is available free of charge via the Internet at http://pubs.acs.org.

JA0676962